Magnetic Nanofilm of Fe₃O₄ for Highly Efficient Organic Light-Emitting Devices

Jing Feng,[†] Dan-Dan Zhang,[†] Yue-Feng Liu,[†] Yu Bai,[†] Qi-Dai Chen,[†] Shi-Yong Liu,[†] and Hong-Bo Sun*,[†,‡]

State Key Laboratory on Integrated Optoelectronics, College of Electronic Science and Engineering, Jilin University, 2699 Qianjin Street, Changchun 130012, China, and College of Physics, Jilin University, 119 Jiefang Road, Changchun 130023, People's Republic of China

We have demonstrated enhanced efficiency from organic light-emitting devices (OLEDs) with Fe₃O₄-coated indium−tin−oxide (ITO) anodes. The current efficiency of the OLEDs with Fe₃O₄/ITO anode is increased by 10.5%, when an external magnetic field is applied. This improvement is ascribed to the magnetic field-induced spin polarization of holes injected through the spin aligner of the Fe₃O₄ film, which results in an enhanced formation ratio of singlet excitons. In addition, Fe₃O₄ is also found acting as an anodic buffer to increase the hole-injection efficiency. The improved luminance and efficiency considered as resulting from the anode interfacial modification of Fe₃O₄ compared to the devices with bare ITO.

Introduction

Organic light-emitting devices (OLED) have attracted much attention due to their application in flat panel display and solid-state lighting.[1,2] Highly efficient fluorescent OLEDs have been reported over the past a few years.[3−5] Even though the fact that the vast majority of organic materials are fluorescent, the development of fluorescent molecules based on OLEDs is a challenging task because of their low quantum efficiency. Emission from triplet excitons is forbidden for fluorescent molecules; therefore, the maximum of internal quantum efficiency of the electroluminescence (EL) remains at 25% for fluorescent OLEDs, due to the 1:3 formation ratio of singlet to triplet excitons. Although a few research works have suggested that the singlet fraction formed in π-conjugated oligomers and polymers may exceed 25%,[6] there has been no result showing that fluorescent small molecules can break through this limit. Increasing the formation ratio of the singlets has been a subject of intensive studies recently. Among them, use of a magnetite electrode as a spin injector under an applied magnetic field was believed to be an effective method to tune the singlet and triplet fraction.[7] The idea has been partially realized, and enhanced EL efficiency and circularly polarized EL from OLEDs have been observed.[8−11] However, most magnetic materials like Fe, Co, and Ni are usually not appropriate either as a cathode of OLEDs due to their relatively high work function or as an anode because of their poor transparency. Therefore, utilization of an appropriate thin magnetite film as a spin aligner instead of an electrode and inserting it between electrodes and organic interface[12] could be a potentially promising method to solve these problems.

In this paper, we chose magnetite Fe₃O₄ film as a promising spin aligner and inserted it between indium−tin−oxide (ITO) anode and the emitting layer of *N,N*′-diphenyl-*N,N*′-bis(1-naphthyl)-(1,1′-biphenyl)-4,4′-diamine (NPB). An enhancement of current efficiency has been achieved through the injection of spin-polarized holes and consequently increased singlet fraction. The ferrimagnetic compound Fe₃O₄ was selected in this work due to its 100% spin polarization, high Curie temperature, and low electrical resistivity at room temperature. The traditional hole-transporting layer, NPB, was used as the emitting layer, and the excitons are expected to be restricted within the NPB layer by using a hole-blocking layer between NPB and the cathode. Therefore, the emission region is confined within the diffusion length of the spin-polarized holes in the emitting layer, usually a few tens of nanometers.[10,12] In addition to the spin injection through the Fe₃O₄ film, hole-injection efficiency is significantly enhanced by using the Fe₃O₄ as the anodic buffer. As a result, the turn-on voltage is largely decreased, and the brightness, the current density, and the efficiency of the OLEDs are highly improved due to the interface modification of Fe₃O₄.

Experimental Details

The device structure was as follows: ITO/Fe₃O₄(*x* nm)/NPB(30 nm)/4,7-diphenyl-1,10-phenanthroline(BPhen, 70 nm)/LiF (0.5 nm)/Al. Here, NPB was utilized as the emitting layer and BPhen as the electron-transporting and hole-blocking layer. Both the Fe₃O₄ and the organic layers were sequentially evaporated by vacuum deposition onto an ITO-coated glass substrate. The X-ray photoelectron spectroscopy (XPS) measurements were performed with Mg Ka X-ray source (1253.6 eV) (Specs XR50). The electroluminescence (EL) spectra of the devices were measured by a PR655 spectroscan spectrometer, and the current density−voltage−luminance (*J−V−L*) characteristics were recorded simultaneously by combining the spectrometer with Keithley model 2400 programmable voltage-current source. The enhancement of the current efficiency (cd/A, η) is defined by their relative difference in the presence and in the absence of a magnetic field (**B**), e. g., $[\eta(\mathbf{B}) - \eta(0)]/\eta(0) = \Delta\eta/\eta$. The 1500 Oe magnetic field was applied perpendicular to the device plane. The field effect on the efficiency was measured by applying and withdrawing a magnet in the interval of 0.5 V of applied voltage, so that the *J−L−V* characteristics with and without the magnetic field can be measured on the same device within the same sequence. The interval data between the measured ones is interpolated from the measured

＊ To whom correspondence should be addressed. E-mail: hbsun@jlu.edu.cn.
　† State Key Laboratory on Integrated Optoelectronics, College of Electronic Science and Engineering, Jilin University.
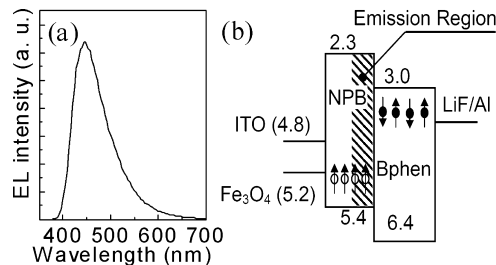　‡ College of Physics, Jilin University.
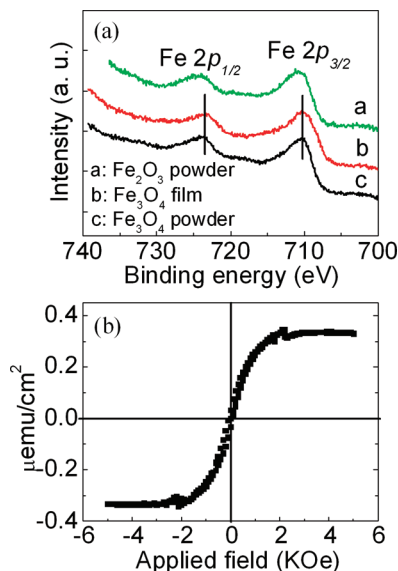
Figure 1. (a) XPS Fe 2p core-level spectrum of the Fe_3O_4 film with those from Fe_3O_4 and Fe_2O_3 powders as reference, and (b) hysteresis loop of an evaporated 70-nm-thick Fe_3O_4 film measured at 300 K. The layer is purposely designed thicker for the convenience of signal detection.

Figure 2. EL spectrum of the OLEDs with NPB as the emitter (a) and energy band diagram of the devices (b).

Figure 3. Enhancement of the efficiency dependent on the thicknesses of the Fe_3O_4 film. Data are mean $\pm$ S. E. (bars) values of four experiments. Where no error bar is shown, the S. E. falls within the size of the symbol. The applied magnetic filed strength is 1500 Oe.

data, and the efficiency curves are then fitted to calculate the enhancement factor. This procedure was performed in order to remove any effects due to the drifting of the devices property and the variation in different devices. All of the measurements were conducted at room temperature.

Results and Discussion

The atomic compositions of the deposited Fe_3O_4 thin films are analyzed by XPS, to which the spectra of Fe_3O_4 and Fe_2O_3 powders are referred. Fe_3O_4 powder was used for the evaporation to deposit the Fe_3O_4 film. Their Fe 2p core-level spectra are shown in Figure 1a. The spectra of Fe_3O_4 thin film (curve b) coincides with that of the powder (curve c) very well, exhibiting typical Fe 2p peaks of Fe_3O_4 at 723.6 and 710.4 eV, whereas the typical Fe 2p peaks of Fe_2O_3 are at 724.1 and 710.7 eV[13] (curve a). Therefore, the thin film deposited by thermal evaporation under high vacuum from Fe_3O_4 powder is confirmed to stoichiometrically consist of Fe_3O_4. Since it has been known that the performance of the magnetite thin film is generally different from that of bulk,[14−16] the evaporated Fe_3O_4 film was characterized by superconducting quantum interference device (SQUID) [Figure 1b]. The hysteresis loop shows that the remanence (0.03 μemu/cm³) and coercivity (<80 Oe) were negligible, and reduced saturation magnetization and the superparamagnetism behavior were obviously seen. The saturated magnetization under room temperature is around 50 emu/cm³ for 70 nm Fe_3O_4 film. The value of the saturated magnetization usually less than that of the bulk (~471 emu/cm³),[17,18] and decreases with the decreasing film thickness for the magnetic thin film. This is proposed due to the increase of the antiphase boundary density,[14,16] and the disorder induced by the thermal evaporation may also contribute to the reduced value in our case.

The EL spectrum of the device exhibits an emission peak at around 440 nm [Figure 2a], which is the characteristic emission of NPB. It shows that the exciton confinement was achieved and emission mainly took place at the NPB layer. The band diagram [Figure 2b] indicates that the Fermi level of Fe_3O_4 (5.2 eV)[19] is between the Fermi level of ITO (4.8 eV) and the HOMO
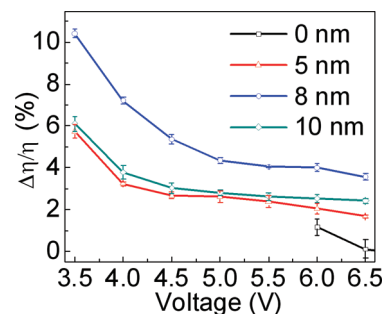
level of NPB (5.4 eV), so that holes will inject from ITO into Fe_3O_4 first, where formation of spin polarized holes due to the strong ferromagnetism of the Fe_3O_4 is expected. Subsequently these spin-polarized holes pass into the emitting layer. It has been predicted that the recombination of injected spin-polarized holes of 100% polarization with nonspin-polarized electrons raises the singlet fraction by 1/3, as leads to 33% EL efficiency enhancement in fluorescent OLEDs.[12]

The efficiency enhancement of the devices shows the Fe_3O_4 layer thickness x-dependent at the applied magnetic field of 1500 Oe as shown in Figure 3. When the Fe_3O_4 layer becomes thicker, x increasing from 0 to 10 nm, $\Delta\eta/\eta$ first increases and then decreases at various applied voltages, and the maximized enhancement of $\Delta\eta/\eta = 10.5\%$ is reached at $x = 8$ nm. It has been reported that the magnetic field influenced the singlet and triplet formation of the OLEDs even though there was no magnetite as spin aligner in OLEDs.[20,21] In the current research, the EL efficiency of the device with 0 nm Fe_3O_4 shows enhancement of 0−1.2% under the same magnetic field and this achieved enhancement is much lower than those from the devices with an optimized Fe_3O_4 thickness. Therefore, the spin regulation of the Fe_3O_4 film to the injected holes should be responsible and it is critical to the EL enhancement. The efficiency enhancement of the devices with different Fe_3O_4 thickness shows clearly applied voltage dependence. The enhancement factors decrease quickly with the increasing of the applied voltage. Further investigations are needed to explain this phenomenon.

The magnetic field-induced effect on the OLEDs with 8 nm Fe_3O_4 is shown in Figure 4. Figure 4a shows the measured current efficiency with an alternate magnetic field. As can be seen, the current efficiency curve is a wave-like shape and shows peaks when a magnetic field is applied. The interval data between the measured ones for both field on and field off measurements is interpolated from the data in Figure 4a and shown in Figure 4b, so that the efficiency enhancement could be obtained through calculating the relative difference of the

6720 *J. Phys. Chem. C, Vol. 114, No. 14, 2010*

Feng et al.
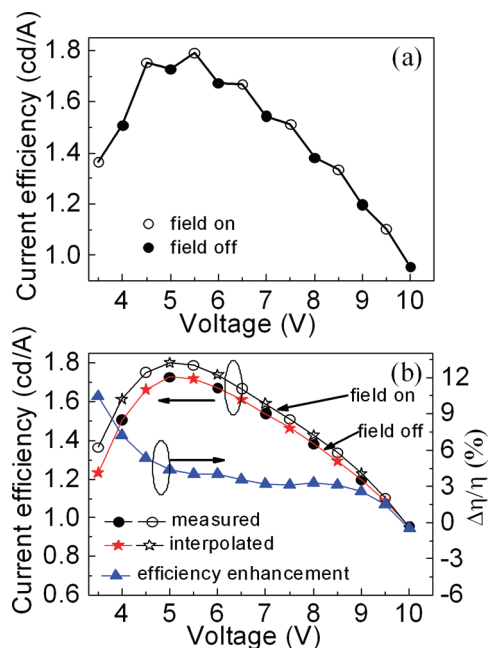
Figure 4. Current efficiency calculated from the measure $J-L-V$ data (a) and fitted in the presence and in the absence of the magnetic field respectively (b). The efficiency enhancement is also shown in (b).

Figure 5. Current density vs voltage (a), luminance vs voltage (b), and current efficiency vs voltage (c) of devices with bare and 8 nm Fe_3O_4 coated ITO anode.

data in the presence and in the absence of the magnetic field, respectively. The enhancement factors also shown in Figure 4b are from 10.5 to 0%, when the applied voltage is increased from 3.5 to 10 V.

It has been demonstrated that a buffer layer inserted between an electrode and an organic layer plays a crucial role in the performance of the OLEDs.[22,23] In the case of the interface between an anode and a hole-transporting layer, transition metal oxides including Fe_3O_4 have shown their effects in hole-injection barrier lowing and interface morphology modification.[24−28] Reduced driving voltage and enhanced luminance, efficiency, and stability have been achieved by introduction of the thin transition metal oxides on the anode. Besides the magnetic-field-induced spin polarization of the injected holes, the efficiency of the injected holes has been increased largely by inserting the magnetic Fe_3O_4 film between the ITO anode and the emitting layer in this OLED structure. The effect of the enhanced hole-injection of the Fe_3O_4 buffer is characterized by comparing the OLEDs with bare and 8 nm Fe_3O_4 coated ITO anodes. The current density and luminance markedly increase for the devices with the Fe_3O_4 coated ITO anode, as shown in Figure 5, panels a and b. The turn-on voltage is reduced from 5 to 3 V. The luminance reaches maximum luminance of 4500 cd/m^2 at 9 V, in contrast to that of only 600 cd/m^2 at 12 V for devices without the Fe_3O_4. The current efficiency [Figure 5c] shows 100% enhancement from 0.9 to 1.8 cd/A. This is by far the highest EL performance obtained from the NPB-based OLEDs.[29] That the data for the devices with the bare ITO shows larger error in Figure 3 is also attributed to it poor EL performance without the anodic modification of the Fe_3O_4 nanofilm.

Conclusion

We have demonstrated the highly improved performance of the OLEDs by using a Fe_3O_4 coated anode. The magnetic Fe_3O_4 thin film plays a dual role as a spin aligner and also as an anodic buffer in improving the performance of OLEDs. In the former case, the singlet exciton fraction is increased due to the
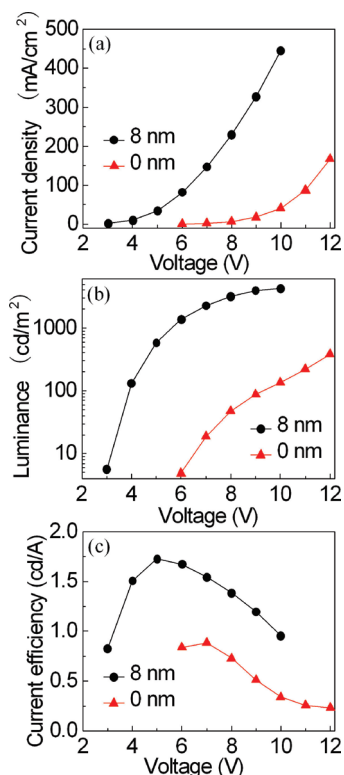
recombination of the spin-polarized holes injected from the Fe_3O_4 coated anode and the nonspin-polarized electrons. In the later case, the holes injection is enhanced by the anodic interfacial modification of Fe_3O_4. Efficiency enhancement of 10.5% due to the spin polarization and 100% due to the anode interfacial modification are achieved for the OLEDs with the Fe_3O_4 coated ITO anode. Although more intensive theoretical and experimental investigations are needed to solidify the role of Fe_3O_4 film as a spin aligner, the observational fact we attained may open a new avenue to the broad application of Fe_3O_4, an environmentally benign, inexhaustible, and cheap material in OLEDs.

References and Notes

(1) Köhler, A.; Wilson, J. S.; Friend, R. H. *Adv. Mater.* **2002**, *14*, 701.
(2) D' Andrade, B. W.; Forrest, S. R. *Adv. Mater.* **2004**, *16*, 1585.
(3) Okumoto, K.; Kanno, H.; Hamaa, Y.; Takahashi, H.; Shibata, K. *Appl. Phys. Lett.* **2006**, *89*, 063504.
(4) Wen, S. W.; Lu, T. H. *SID Symp. Dig.* **2004**, *35*, 784.
(5) Hancock, J. M.; Gifford, A. P.; Tonzola, C. J.; Jenekhe, S. A. *J. Phys. Chem. C* **2007**, *111*, 6875.
(6) Wohlgenannt, M.; Tandon, K.; Mazumdar, S.; Ramasesha, S.; Vardeny, Z. V. *Nature* **2001**, *409*, 494.
(7) Ruden, P. O.; Smith, D. L. *J. Appl. Phys.* **2004**, *95*, 4898.
(8) Wilkinson, J.; Davis, A. H.; Bussmann, K.; Long, J. P. *Appl. Phys. Lett.* **2005**, *86*, 111109.
(9) Shikoh, E.; Kawai, T.; Fujiwara, A.; Ando, Y.; Miyazaji, T. *J. Magn. Magn. Mater.* **2007**, *310*, 2052.
(10) Shikoh, E.; Fujiwara, A.; Ando, Y.; Miyazaki, T. *Jpn. J. Appl. Phys.* **2006**, *45*, 6897.
(11) Wu, D.; Xiong, Z. H.; Li, X. G.; Vardeny, Z. V.; Shi, J. *Phys. Rev. Lett.* **2005**, *95*, 016802.
(12) Wu, Y.; Hu, B.; Howe, J.; Li, A. P.; Shen, J. *Phys, Rev. B* **2007**, *75*, 075413.

(13) Kim, K. J.; Moon, D. W.; Lee, S. K.; Jung, K. H. *Thin Solid Films* **2000**, *360*, 118.

(14) Arisi, E.; Bergenti, I.; Cavallini, M.; Riminucci, A.; Ruani, G.; Dediu, V.; Ghidini, M.; Pernechele, C.; Solzi, M. *Appl. Phys. Lett.* **2008**, *93*, 113305.

(15) Voogt, F. C. M.; Palstra, T. T.; Niesen, L.; Rogojanu, O. C.; James, M. A.; Hibma, T. *Phys. Rev. B* **1998**, *57*, R8107.

(16) Eerenstein, W.; Hibma, T.; Celotto, S. *Phys. Rev. B* **2004**, *70*, 184404.

(17) Bickford, L. R., Jr. *Phys. Rev.* **1950**, *78*, 449.

(18) Kale, S.; Bhagat, S. M.; Lofland, S. E.; Scabarozi, T.; Ogale, S. B.; Orozco, A.; Shinde, S. R.; Venkatesan, T.; Hannoyer, B.; Mercey, B.; Prellier, W. *Phys. Rev. B* **2001**, *64*, 205413.

(19) Fonin, M.; Pentcheva, R.; Dedkov, Y. S.; Sperlich, M.; Vyalikh, D. V.; Scheffler, M.; Rüdiger, U.; Güntherodt, G. *Phys. Rev. B* **2005**, *72*, 104436.

(20) Odaka, H.; Okimoto, Y.; Yamada, T.; Okamoto, H.; Kawasaki, M.; Tokura, Y. *Appl. Phys. Lett.* **2006**, *88*, 123501.

(21) Kalinowski, J.; Cocchi, M.; Virgili, D.; Marco, P. D.; Fattori, V. *Chem. Phys. Lett.* **2003**, *380*, 710.

(22) Shen, Y. L.; Jacobs, D. B.; Malliaras, G. G.; Koley, G.; Spencer, M. G.; Ioannidis, R. *Adv. Mater.* **2001**, *13*, 1234.

(23) Hung, L. S.; Tang, C. W.; Mason, M. G.; Raychaudhuri, P.; Madathil, J. *Appl. Phys. Lett.* **2001**, *78*, 544.

(24) You, H.; Dai, Y.; Zhang, Z.; Ma, D. *J. Appl. Phys.* **2007**, *101*, 026105.

(25) Hu, W.; Manabe, K.; Furukawa, T.; Matsumura, M. *Appl. Phys. Lett.* **2002**, *80*, 2640.

(26) Chan, I. M.; Hsu, T. Y.; Hong, F. C. *Appl. Phys. Lett.* **2002**, *81*, 1899.

(27) Duan, L.; Liu, Q.; Li, Y.; Gao, Y.; Zhang, G.; Zhang, D.; Wang, L.; Qiu, Y. *J. Phys. Chem. C* **2009**, *113*, 13386.

(28) Zhang, D. D.; Feng, J.; Liu, Y. F.; Zhong, Y. Q.; Bai, Y.; Jin, Y.; Xie, G. H.; Xue, Q.; Zhao, Y.; Liu, S. Y.; Sun, H. B. *Appl. Phys. Lett.* **2009**, *94*, 223306.

(29) Divayana, Y.; Sun, X. W.; Chen, B. J.; Lo, G. Q.; Jiang, C. Y.; Sarma, K. R. *Appl. Phys. Lett.* **2006**, *89*, 173511.